

Enantioselective Pd-Catalyzed Electrochemical Dearomative Allylation of Tropones: Construction of All-C Quaternary Stereocenters

Giulia Monda, Sofia Kiriakidi, Olalla Nieto Faza,* Andrea Mazzanti, Giulio Bertuzzi,* and Marco Bandini*



Cite This: *Org. Lett.* 2026, 28, 4227–4233



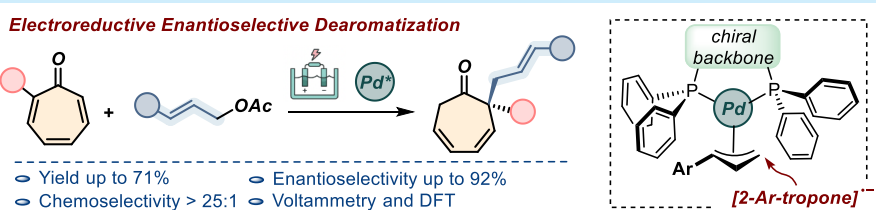
Read Online

ACCESS |

Metrics & More

Article Recommendations

Supporting Information



ABSTRACT: A Pd-catalyzed electroreductive enantioselective dearomatization of tropones is documented. High levels of chemoselectivity toward the formation of seven-membered ring ketones featuring a stereochemically controlled all-carbon α -stereocenter are successfully accomplished by means of a Tsuji–Trost-like process (24 examples, regioselectivity >25:1, *enantiomeric ratio* of up to 96:4). Computational and electrochemical analyses allowed elucidation of the reaction manifold that involves initial reduction of the troponone motif and a subsequent chemo- and enantioselective allylation via an outer-sphere approach. In this way, a novel concept for the dearomatization of electron-poor scaffolds is disclosed by means of electrochemical reductive umpolung.

The growing interest in discovering new reaction manifolds that leverage electrochemistry can be attributed to the *in situ* reversal of the classical reactivity of a given compound through electron-transfer processes.¹ Electrosynthesis is thus revolutionizing the horizons of synthetic organic chemistry, not only by transforming outdated and environmentally detrimental methodologies into sustainable alternatives,² but also by enabling novel reactivity modes in which certain classes of compounds undergo transformations that would otherwise be inaccessible through conventional pathways. This advancement broadens the scope and overcomes the limitations of well-established and robust synthetic protocols.

Within this context, the field of enantioselective dearomatizations, which aims to construct complex, optically active three-dimensional architectures from planar two-dimensional chemical spaces, has now reached an exceptional level of maturity,³ and these processes serve as a key strategy underpinning the current “escape from flatland” paradigm in medicinal chemistry.⁴

However, the field of dearomatization reactions still poses a significant synthetic challenge, as it remains largely dominated by electron-rich arenes and heteroarenes (e.g., indoles, pyrroles, naphthols, phenols, etc.). These scaffolds typically offer favorable energetic profiles and enable mild and selective reaction conditions to be applied.⁵ In contrast, the involvement of electron-deficient arenes has been restricted to few isolated

examples of dearomative transformations of specific pyridine derivatives,⁶ leaving substantial room for further development.

Here, we envisioned that the implementation of electrochemical methodologies could expand this chemical space by enabling electron-deficient species to participate in the target transformation, being turned into electron-rich intermediates through site-selective reductive electron-transfer processes.⁷ Remarkably, the use of electrochemistry in enantioselective dearomatizations remains unexplored to date.⁸

Our interest in discovering new electrochemical organic transformations⁹ led to the investigation of the still largely unexplored redox chemistry profiles of troponone/tropolone derivatives.¹⁰ In this direction, an example of *in situ* chemical umpolung (electrophile \rightarrow nucleophile) was recently disclosed as a productive strategy to realize an electroreductive Ni-catalyzed alkylation of the aromatic core of troponone.^{10c}

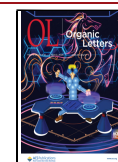
In line with these recent findings and the aforementioned working hypothesis, we herein present a new strategy toward a direct asymmetric electro-dearomatization of electron-poor

Received: February 14, 2026

Revised: March 6, 2026

Accepted: March 13, 2026

Published: March 18, 2026



arenes (i.e., tropones) through condensation with electrophilic allyl–metal species.¹¹ This approach draws inspiration from the well-established α -allylation of ketones that is commonly carried out via pre-enolization under basic conditions (Figure 1, top).¹² Alternatively, although less explored, the same

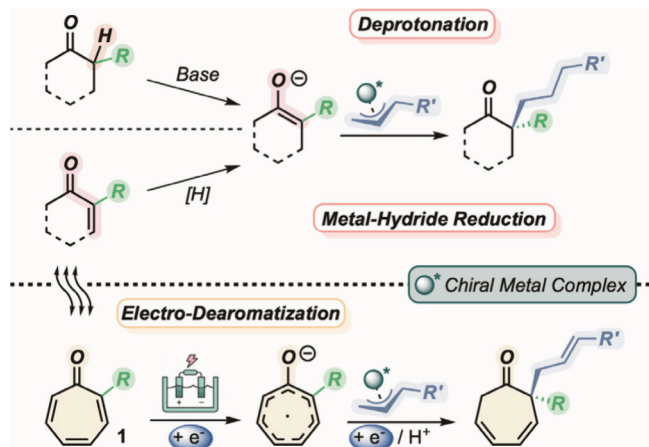


Figure 1. Introducing the concept of electro-dearomatization as reactivity umpolung of tropones. Previous modes of enolate generation toward enantioselective Tsuji–Trost allylations (top). Present working hypothesis addressing a metal-catalyzed electrochemical dearomative protocol (bottom).

process can involve the *in situ* formation of metal enolates, via conjugate hydride addition to electron-poor olefins (Figure 1, center).¹³ By recognizing the intrinsic structural analogy between α,β -unsaturated carbonyls and the troponone scaffold,

we envisioned that the desired electrophile-to-nucleophile reactive inversion on the troponone core could be realized through electrochemical reduction of the seven-membered ring.

The realized “enolate-like” radical ion might be conveniently engaged in an asymmetric allylation strategy (Tsuji–Trost-like process)¹⁴ to generate rapid access to densely functionalized cyclic scaffolds in enantiomerically enriched form. It is worth mentioning that our working plan would replace the use of strongly basic environments or harmful hydride sources with green electrons, enabling the reductive pathway.

Additionally, the adoption of the sacrificial anode strategy would preclude any oxidative rearomatization, leading to a fully reductive dearomatizing pathway (Figure 1, bottom). Furthermore, we foresee that the use of 2-substituted tropones **1** would potentially address the formation of synthetically challenging all-carbon quaternary stereogenic centers,¹⁵ in agreement with the enantioselective allylation of α -mono-substituted cyclic ketones.¹⁶

At the outset of our investigation, we tackled our working hypothesis by reacting 2-phenyltroponone **1a** and cinnamyl acetate **2a** in the presence of $[\text{PdCl}_2(\text{acn})_2]$ and the Trost-type ligand **L1**. Importantly, the structure of **2a** was selected in order to challenge the linear and branched selectivity of our methodology. Electrochemical conditions involved the use of a sacrificial anode (Zn), a Ni cathode, and constant current electrolysis (10 mA, 1.5 h, TEABF₄ electrolyte) in an ACN/MeOH (5:1) solvent mixture.¹⁷ Under these conditions, compound (*S*)-**3aa** was isolated in low yet promising yield (22%) and *enantiomeric ratio* (65:35 (Table 1, entry 1)). Remarkably, only the regioisomer featuring an all-carbon

Table 1. Optimization of the Reaction Conditions^a

| entry | L | solvent | electrode ((-) (+)) | additive | T (°C) | yield of 3aa ^b (%) | er of 3aa ^c |
|-------------------|------|---------------|----------------------|--|--------|--------------------------------------|-------------------------------|
| 1 | L1 | 5:1 ACN/MeOH | Ni Zn | – | 25 | 22 | 65:35 |
| 2 | L2 | 5:1 ACN/MeOH | Ni Zn | – | 25 | 36 | 55:45 |
| 3 | L3 | 5:1 ACN/MeOH | Ni Zn | – | 25 | 22 | 55:45 |
| 4 | L4–7 | 5:1 ACN/MeOH | Ni Zn | – | 25 | NR | – |
| 5 ^d | L1 | 5:1 THF/MeOH | Ni Zn | – | 25 | 26 | 72:28 |
| 6 ^d | L1 | 60:1 THF/MeOH | Ni Zn | – | 25 | 62 | 78:22 |
| 7 ^d | L1 | 60:1 THF/MeOH | Ni Zn | – | 0 | 47 | 85:15 |
| 8 ^{d,e} | L1 | 60:1 THF/MeOH | Ni Zn | TBACl (1 equiv) | 0 | 25 | 92:8 |
| 9 ^{d,e} | L1 | 60:1 THF/MeOH | W Zn | TBACl (1 equiv) | 0 | 31 | 94:6 |
| 10 ^{d,e} | L1 | 60:1 THF/MeOH | W Mg | TBACl (1 equiv) | 0 | 27 | 85:15 |
| 11 ^{d,e} | L1 | THF | W Zn | H ₂ O (12 equiv), TBACl (1 equiv) | 0 | 62 | 94:6 |

^aAll reactions were carried in the Electrasyn 2.0 apparatus (3:1 **1a**:**2a**, 0.3 M **2a**, TEABF₄ electrolyte). ^bIsolated yields after flash chromatography.

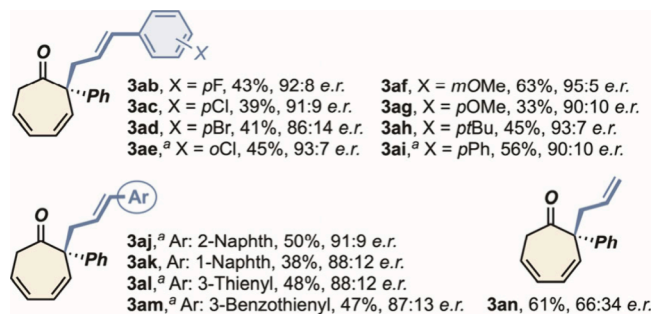
^cDetermined by chiral HPLC analysis. ^dThe TBAPF₆ electrolyte was used for better solubility. ^eT = 5 mA; 3 h. NR: no reaction.

quaternary stereogenic center was detected in the reaction mixture, with the allyl moiety exclusively in the linear form. Other ligands, as well as Pd sources, proved to be far less efficient in terms of stereocontrol and isolated yield (entries 2–4 and Supporting Information). Changing the solvent from acetonitrile to THF led to an increase in the *enantiomeric ratio* to up to 78:22 (entry 5). The quantity of the protic source (i.e., MeOH) was also pivotal for the chemical outcome,¹⁸ and when the amount was decreased to 60:1 THF/MeOH, the yield and enantioselectivity were both improved (entry 6). Finally, with a decrease in the temperature to 0 °C, **3aa** was obtained in 85:15 *er* (entry 7).¹⁹

To further optimize the enantioselectivity of the process, the use of TBACl as an additive was tested, given the well-established positive role of halide ions in the enantioinduction of Tsuji–Trost allylations.²⁰ Remarkably, although a decrease in efficiency (25% yield) was recorded, **3aa** was isolated in a 92:8 *enantiomeric ratio* (entry 8). These conditions prompted us to undertake an intense survey of different electrode couples, resulting in a slight improvement in the isolated yield and *enantiomeric ratio* upon replacement of Ni with W as the cathode (31%; see also the Supporting Information). Finally, upon a final screening of protic sources (see the Supporting Information and *vide infra* for mechanistic elucidations), we discovered water to be the most efficient, allowing **3aa** to be isolated in 62% yield and 94:6 *er* (entry 11).²¹

Thereafter, the scope of the reaction was initially investigated by testing a series of cinnamyl acetates (**2b–n**), and the results are listed in Scheme 1. The introduction of

Scheme 1. Testing Different Cinnamyl Acetates 2 (reaction conditions from entry 11 of Table 1)



^aAt a 6:1 **1a**:**2** ratio with a reaction time of 6 h.

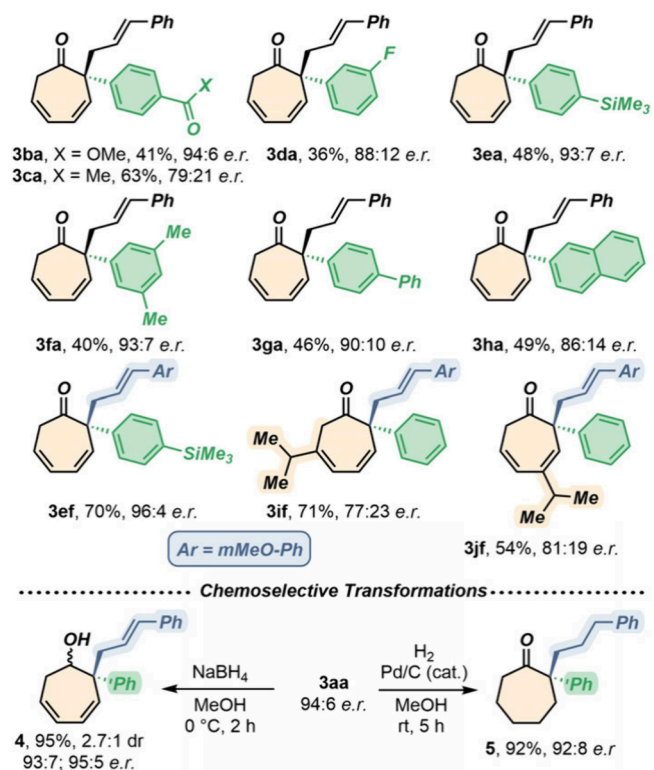
halogen atoms at the *para* and *ortho* positions of the cinnamyl aryl unit (**2b–e**) led to constantly high *enantiomeric ratios* (up to 93:7, **3ae**) and moderate isolated yields. Even higher levels of enantiocontrol were achieved by employing allylating agents based on EDG-substituted acetates (**2f–i**). Here, an *enantiomeric ratio* as high as 96:4 was recorded with the precursor carrying a *m*MeO-substituted arene, together with a synthetically useful 63% isolated yield (**3af**). The compatibility of the protocol toward different allylating units was also ascertained with the exploration of extended as well as heteroarene derivatives (**2j–m**). Satisfyingly, moderate to high *enantiomeric ratios* were always accompanied by reasonably high isolated yields (up to 51%, **3am**). However, when simple allyl acetate **2n** was employed, cycloheptadienone **3an** was isolated with low optical purity, although in a good yield.

Then, our attention turned to assessing the generality of the protocol toward the decoration of the tropono scaffold. In this direction, a series of α -substituted tropones were synthesized via Suzuki–Miyaura cross-coupling (**1b–k**).

Remarkably, the regioselectivity toward the targeted quaternary stereogenic center was always recorded, with no trace of the dearomatized C(7)-allylated isomer (Scheme 1, top). Here, a wide range of functional groups could be accommodated at the tropono moiety, such as halides (**1d**), esters (**1b**), ketones (**1c**), alkyl and aryl groups (**1f** and **1g**), silyl moieties (**1e**), and extended π -systems (**1h**). In this context, isolated yields and *enantiomeric ratios* reached 70% and 96:4, respectively, in the case of compound **3ef**. Finally, isomeric 4- and 6-isopropyl-2-phenyl-tropones **1j** and **1k**, which could be divergently obtained from the same chemical source (i.e., β -thujapicin), were subjected to the present Pd-catalyzed enantioselective reductive dearomatization, leading to moderate *enantiomeric ratios* and good yields.

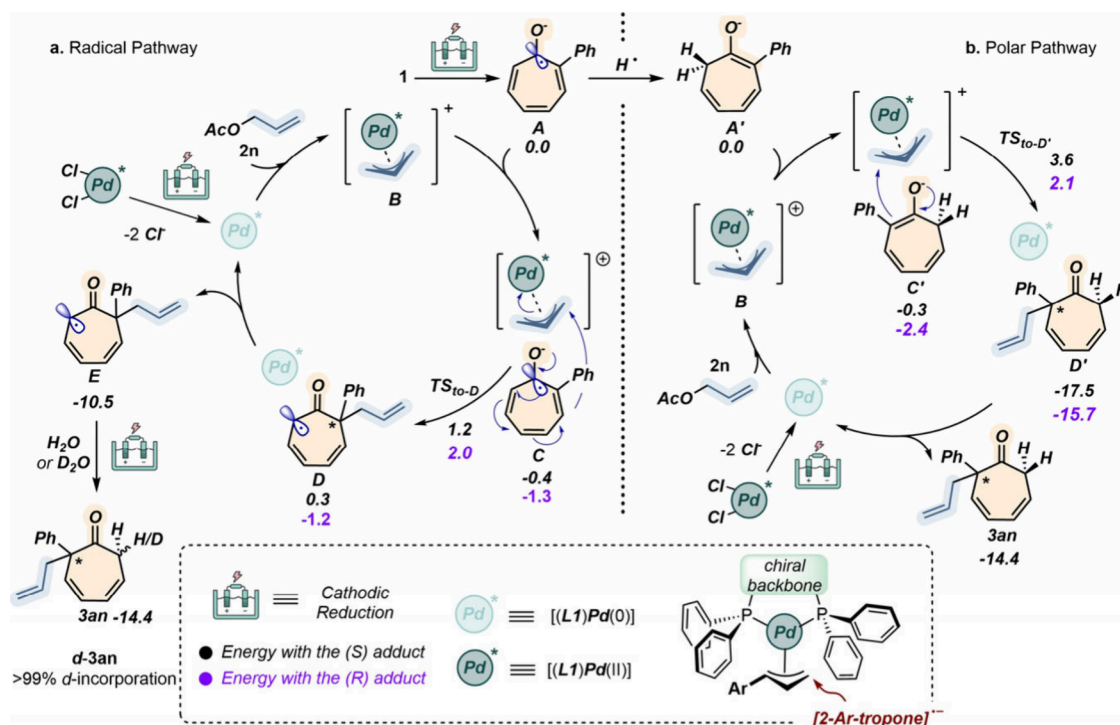
Finally, to access the versatility of products **3** toward chemical manipulation, we tackled two chemoselective reductions of **3aa** (Scheme 2, bottom). First, transformation

Scheme 2. Testing Different 2-Aryltropones 1 (top, reaction conditions from entry 11 of Table 1) and Chemoselective Reduction of Dearomatized Cycloheptadienones **3aa** (bottom)



of the ketone moiety (NaBH_4) toward alcohol **4** was realized in excellent yield (95%), moderate diastereoselectivity (2.7:1), and high retention of the starting *enantiomeric ratio*. Alternatively, the three double bonds of **3aa** could be hydrogenated to fully saturated product **5**, retaining the carbonyl function, in excellent yield (92%), with good retention of enantioselectivity.

In order to gain a deeper mechanistic understanding of the studied reaction, we employed DFT calculations at the

Scheme 3. Proposed Mechanistic Pathways for the Pd-Catalyzed Electrochemical Dearomative Allylation of Troponone 1^a

^aThe reported energies correspond to ΔG values in kilocalories per mole.

r^2 SCAN/def2-SV(P)/THF(CPCM) level,²² using THF as the solvent (see the Supporting Information for further details). The computational study is based on the results obtained from a voltametric investigation carried out on 2-phenyl-troponone **1a** and the preformed $[Pd(PPh_3)_2(\eta^3\text{-allyl})]BF_4$ complex (Figure S8).²³ These clearly indicate that reduction of **1a** occurs preferentially (-1.80 V vs Fc/Fc^+) with respect to the Pd complex (-2.42 V vs Fc/Fc^+), suggesting an unlikely formation of low-valent allyl–Pd intermediates and pointing toward the electrochemical generation of nucleophilic species from the reduction of **1a**. We therefore propose an initial reduction of precomplex $[(L1)Pd(II)Cl_2]$ to catalytically active $[(L1)Pd(0)]$ that can add to allyl acetate **2n** to give $[Pd(L1)(\eta^3\text{-allyl})]$ complex **B**.²⁴ At the same time, **1a** is reduced at the cathode to generate radical anion **A**. We then performed the mechanistic study by considering two alternative pathways featuring species **A** as a common initial precursor (Scheme 3).

In particular, pathway a) relies on a direct electrodearomatization step directly involving radical anion **A** and its condensation with *in situ*-formed $[Pd(L1)(\eta^3\text{-allyl})]$ complex **B**. Here, weakly stabilized precomplex **C** is formed where the allyl unit approaches the carbon *ipso* to the Ph group. Both diastereomeric transition states were identified and compared from an energetic viewpoint. Interestingly, the (S)-TS (**C** \rightarrow **D**) exhibits an activation energy (1.6 kcal/mol) lower than that of the one leading to the R enantiomer (3.3 kcal/mol). This finding matches the determination of the absolute configuration of the major isomer (see the Supporting Information for details) and aligns closely with the experimental observation that, with a decrease in the temperature to 0 °C, enhanced enantioselectivity was achieved (entry 6 vs entry 7, Table 1). Next, the loosely bound reduced Pd complex (**D**) dissociates leading to thermodynamically

stable radical **E**. The latter was then easily quenched through reduction and protonation to yield product **3an**. The active role played by water in the final proton quenching was proved by running the model process in the presence of D_2O as the additive. Here complete monodeuteration was detected at C-7 of the cycloheptadienyl ring.

In pathway b), we first assumed that radical anion **A** could be quenched through a HAT event, yielding **A'**, which then reacts with $[Pd(L1)(\eta^3\text{-allyl})]$ **B** leading to precomplex **C'**. The following rate-determining reductive elimination takes place with activation energies of 3.9 and 4.4 kcal/mol for the S and R enantiomers, respectively. Resulting intermediate **D'** was quite stable for both isomers, and the subsequent release of the catalyst leading to final product **3an** was found to be uphill by 2–4 kcal/mol. Both the kinetics of the rate-determining step and the thermodynamics of catalyst release suggest that radical pathway a) is most likely the mechanistic route followed by the present transformation. It is worth noting that this allylation occurs through an outer-sphere approach. In fact, all attempts to compute reaction machineries involving coordination of the Pd catalyst to the troponone core before C–C bond formation led to remarkably higher (10 kcal/mol) energy barriers for the transition states (see Figure S9). Finally, we were able to rationalize the stereoselection experimentally recorded (S enantiomer as the major one) that correlated to the key interactions between the aromatic rings of the 2-(diphenylphosphino) benzoic acid amide scaffold of **L1** and the phenyl substituent of the troponone (see Figure S10).

In conclusion, a new strategy for the electroreductive enantioselective dearomatization of 2-aryltropones via a palladium-catalyzed nucleophilic allylic alkylation is presented. The protocol employs chiral C_2 -symmetric Trost-type palladium complexes, enabling rapid access to enantiomerically enriched seven-membered ring ketones bearing all-carbon

quaternary stereogenic centers. The proposed mechanistic rationale (electrochemical enolization of tropone followed by outer-sphere-type allylation) is supported by both experimental (voltametric) and computational (DFT) studies.

■ ASSOCIATED CONTENT

Data Availability Statement

The data underlying this study are available in the published article and in its [Supporting Information](#).

Supporting Information

The Supporting Information is available free of charge at <https://pubs.acs.org/doi/10.1021/acs.orglett.6c00796>.

Experimental procedures, characterization details (copies of NMR spectra and HPLC chromatogram), mechanistic studies, and additional computational details ([PDF](#))

■ AUTHOR INFORMATION

Corresponding Authors

Olalla Nieto Faza – Departamento de Química Orgánica, Universidade de Vigo, 36310 Vigo, Spain; Email: faza@uvigo.gal

Giulio Bertuzzi – Dipartimento di Chimica “Giacomo Ciamician”, Alma Mater Studiorum, Università di Bologna, 40129 Bologna, Italy; Center for Chemical Catalysis, C3 Alma Mater Studiorum, Università di Bologna, 40129 Bologna, Italy; Email: giulio.bertuzzi2@unibo.it

Marco Bandini – Dipartimento di Chimica “Giacomo Ciamician”, Alma Mater Studiorum, Università di Bologna, 40129 Bologna, Italy; Center for Chemical Catalysis, C3 Alma Mater Studiorum, Università di Bologna, 40129 Bologna, Italy; orcid.org/0000-0001-9586-3295; Email: marco.bandini@unibo.it

Authors

Giulia Monda – Dipartimento di Chimica “Giacomo Ciamician”, Alma Mater Studiorum, Università di Bologna, 40129 Bologna, Italy; Center for Chemical Catalysis, C3 Alma Mater Studiorum, Università di Bologna, 40129 Bologna, Italy

Sofia Kiriakidi – Dipartimento di Chimica “Giacomo Ciamician”, Alma Mater Studiorum, Università di Bologna, 40129 Bologna, Italy; Center for Chemical Catalysis, C3 Alma Mater Studiorum, Università di Bologna, 40129 Bologna, Italy

Andrea Mazzanti – Center for Chemical Catalysis, C3 Alma Mater Studiorum, Università di Bologna, 40129 Bologna, Italy; Dipartimento di Chimica Industriale “Toso Montanari”, Alma Mater Studiorum, Università di Bologna, 40129 Bologna, Italy; orcid.org/0000-0003-1819-8863

Complete contact information is available at:

<https://pubs.acs.org/doi/10.1021/acs.orglett.6c00796>

Notes

The authors declare no competing financial interest.

■ ACKNOWLEDGMENTS

The authors are grateful to the University of Bologna for financial support and Project PRIN-2022 (20227Z3BL8). M.B. is also grateful to Consorzio CINMPIS. O.N.F. and S.K. thank

the Xunta de Galicia for funding through the fellowship “Ayudas de apoyo a la etapa de formación posdoctoral (ED481B-2023-044)” and the “ayudas para a consolidación y estruturación de unidades de investigación competitivas” (ED431B 2025/47). O.N.F. and S.K. are grateful to the Centro de Supercomputación de Galicia for HPC resources and to MICINN (PID2020-115789GB-C22) for research funds. S.K. also thanks the CINECA award under the ISCR initiative for the availability of high-performance computing resources and support.

■ REFERENCES

- (1) (a) Francke, R.; Little, R. D. Redox catalysis in organic electrosynthesis: basic principles and recent developments. *Chem. Soc. Rev.* **2014**, *43*, 2492–2510. (b) Wiebe, A.; Gieshoff, T.; Möhle, S.; Rodrigo, E.; Zirbes, M.; Waldvogel, S. R. Electrifying organic synthesis. *Angew. Chem., Int. Ed.* **2018**, *57*, 5594–5619. (c) Horn, E. J.; Rosen, B. R.; Baran, P. S. Synthetic organic electrochemistry: an enabling and innately sustainable method. *ACS Cent. Sci.* **2016**, *2*, 302–308. (d) Novaes, L. F. T.; Liu, J.; Shen, Y.; Lu, L.; Meinhardt, J. M.; Lin, S. Electrocatalysis as an enabling technology for organic synthesis. *Chem. Soc. Rev.* **2021**, *50*, 7941–8002. (e) Zhu, C.; Ang, N. W.; Meyer, T. H.; Qiu, Y.; Ackermann, L. Organic electrochemistry: molecular syntheses with potential. *ACS Cent. Sci.* **2021**, *7*, 415–431. (f) Wang, Y.; Dana, S.; Long, H.; Xu, Y.; Li, Y.; Kaplaneris, N.; Ackermann, L. Electrochemical late-stage functionalization. *Chem. Rev.* **2023**, *123*, 11269–11335. (g) Zeng, W.; Wang, Y.; Peng, C.; Qiu, Y. Organo-mediator enabled electrochemical transformations. *Chem. Soc. Rev.* **2025**, *54*, 4468–4500.
- (2) (a) Lehnerr, D.; Chen, L. Overview of recent scale-ups in organic electrosynthesis (2000–2023). *Org. Process. Res. Dev.* **2024**, *28*, 338–366. (b) Ferretti, A. C.; Cohen, B.; Deng, L.; Diwan, M.; Frederick, M. O.; Lehnerr, D. Adoption of electrochemistry, within the pharmaceutical industry: insights from an industry-wide survey. *Org. Process Res. Dev.* **2025**, *29*, 322–332.
- (3) (a) You, S.-L., Ed. *Asymmetric dearomatization reactions*; Wiley-VCH: Weinheim, Germany, 2016. (b) Zhuo, C.-X.; Zhang, W.; You, S.-L. Catalytic asymmetric dearomatization reactions. *Angew. Chem., Int. Ed.* **2012**, *51*, 12662–12686. (c) Ding, Q.; Zhou, X.; Fan, R. Recent advances in dearomatization of heteroaromatic compounds. *Org. Biomol. Chem.* **2014**, *12*, 4807–4815. (d) Wu, W.-T.; Zhang, L.; You, S.-L. Catalytic asymmetric dearomatization (CADA) reactions of phenol and aniline derivatives. *Chem. Soc. Rev.* **2016**, *45*, 1570–1580. (e) Zheng, C.; You, S.-L. Catalytic asymmetric dearomatization by transition-metal catalysis: a method for transformations of aromatic compounds. *Chem.* **2016**, *1*, 830–857. (f) Zheng, C.; You, S. L. Advances in catalytic asymmetric dearomatization. *ACS Cent. Sci.* **2021**, *7*, 432–444.
- (4) (a) Lovering, F.; Bikker, J.; Humblet, C. Escape from flatland: increasing saturation as an approach to improving clinical success. *J. Med. Chem.* **2009**, *52*, 6752–6756. (b) Lovering, F. Escape from flatland 2: complexity and promiscuity. *MedChemCommun.* **2013**, *4*, 515–519.
- (5) (a) Zhuo, C.-X.; Liu, W.-B.; Wu, Q.-F.; You, S.-L. Asymmetric dearomatization of pyrroles via Ir-catalyzed allylic substitution reaction: enantioselective synthesis of spiro-2H-pyrroles. *Chem. Sci.* **2012**, *3*, 205–208. (b) Nemoto, T.; Zhao, Z.; Yokosaka, T.; Suzuki, Y.; Wu, R.; Hamada, Y. Palladium-catalyzed intramolecular ipso-Friedel-Crafts alkylation of phenols and indoles: rearomatization-assisted oxidative addition. *Angew. Chem., Int. Ed.* **2013**, *52*, 2217–2220. (c) Zhuo, C.-X.; You, S.-L. Palladium-catalyzed intermolecular asymmetric allylic dearomatization reaction of naphthol derivatives. *Angew. Chem., Int. Ed.* **2013**, *52*, 10056–10059. (d) Xu, Q.-L.; Dai, L.-X.; You, S.-L. Diversity oriented synthesis of indole-based periannulated compounds via allylic alkylation reactions. *Chem. Sci.* **2013**, *4*, 97–102. (e) Zhuo, C.-X.; Zhou, Y.; You, S.-L. Highly regio- and enantioselective synthesis of polysubstituted 2H-pyrroles via Pd-catalyzed intermolecular asymmetric allylic dearomatization of

- pyrroles. *J. Am. Chem. Soc.* **2014**, *136*, 6590–6593. (f) Trost, B. M.; Bai, W.-J.; Hohn, C.; Bai, Y.; Cregg, J. J. Palladium-catalyzed asymmetric allylic alkylation of 3-substituted 1*H*-indoles and tryptophan derivatives with vinylcyclopropanes. *J. Am. Chem. Soc.* **2018**, *140*, 6710–6717. (g) Wang, Y.; Zhang, W.-Y.; Xie, J.-H.; Yu, Z.-L.; Tan, J.-H.; Zheng, C.; Hou, X.-L.; You, S.-L. Enantioselective desymmetrization of bisphenol derivatives via Ir-catalyzed allylic dearomatization. *J. Am. Chem. Soc.* **2020**, *142*, 19354–19359. (h) Zhang, X.; Han, L.; You, S.-L. Ir-catalyzed intermolecular asymmetric allylic dearomatization reaction of indoles. *Chem. Sci.* **2014**, *5*, 1059–1063. (i) Shen, D.; Chen, Q.; Yan, P.; Zeng, X.; Zhong, G. Enantioselective dearomatization of naphthol derivatives with allylic alcohols by cooperative iridium and Brønsted acids catalysis. *Angew. Chem., Int. Ed.* **2017**, *56*, 3242–3246. (j) Cheng, Q.; Xie, J.-H.; Weng, Y.-C.; You, S.-L. Pd-catalyzed dearomatization of anthranils with vinyl-cyclopropanes by [4 + 3] cyclization reaction. *Angew. Chem., Int. Ed.* **2019**, *58*, 5739–5743.
- (6) (a) Min, X.-L.; Zhang, X.-L.; Yi, W.; He, Y. Brønsted acid-enhanced copper-catalyzed atroposelective cycloisomerization to axially chiral arylquinolizones via dearomatization of pyridine. *Nat. Commun.* **2022**, *13*, 373. (b) Greßes, S.; Süße, L.; Casselman, T.; Stoltz, B. M. Tandem dearomatization/enantioselective alkylation of pyridines. *J. Am. Chem. Soc.* **2023**, *145*, 11907–11913. (c) Comparini, L. M.; Pineschi, M. Recent progresses in the catalytic stereoselective dearomatization of pyridines. *Molecules* **2023**, *28*, 6186. (d) Escolano, M.; Gaviña, D.; Alzuet-Piña, G.; Díaz-Oltra, S.; Sánchez-Roselló, M.; del Pozo, C. Recent strategies in the nucleophilic dearomatization of pyridines, quinolines, and isoquinolines. *Chem. Rev.* **2024**, *124*, 1122–1246. (e) Lv, S.; Zhang, G.; Chen, J.; Gao, W. Electrochemical dearomatization: evolution from chemicals traceless electrons. *Adv. Synth. Catal.* **2020**, *362*, 462–477. and references therein
- (7) (a) Wang, K.; Tian, Y.; Li, B.; Wang, L.; Gao, W.; Jia, X.; Wang, R.; Zhu, Y.; Chen, J. Catalyst-free electrochemical dearomatization of pyridine derivatives. *Green Synth. Catal.* **2024**, *5*, 136–139. (b) Sarkar, S.; Rohit; Meanwell, M. W. A chemoselective electrochemical birch carboxylation of pyridines. *Green Chem.* **2025**, *27*, 2900–2906.
- (8) (a) Chang, X.; Zhang, Q.; Guo, C. Asymmetric electrochemical transformations. *Angew. Chem., Int. Ed.* **2020**, *59*, 12612–12622. (b) Jiang, X.; Zou, C.; Zhuang, W.; Li, R.; Yang, Y.; Yang, C.; Xu, X.; Zhang, L.; He, X.; Yao, Y.; Sun, X.; Hu, W. Asymmetric electrochemical synthesis: emerging catalytic strategies and mechanistic insights. *Green Chem.* **2025**, *27*, 915–944. (c) Mo, K.; Zhou, X.; Wu, J.; Zhao, Y. Manganese-mediated electrochemical dearomatization of indoles to access 2-azido spirocyclic indolines. *J. Org. Chem.* **2022**, *87*, 16106–16110. (d) Bag, R.; Mishra, N. P.; Saha, D.; Banerjee, P. Electrochemical oxidative dearomatization strategy for accessing spiro[4.5]dienones and derivatives. *J. Org. Chem.* **2024**, *89*, 2200–2211. (e) Sarvi Beigbaghlou, S.; Yafele, R. S.; Kalek, M. Electrochemical oxidative dearomatization strategy for accessing spiro[4.5]dienones and derivatives. *Synthesis* **2023**, *55*, 4173–4180. (f) Tomczyk, I.; Kalek, M. Electrochemical dearomatizing methoxylation of phenols and naphthols: synthetic and computational studies. *Chem. - Eur. J.* **2024**, *30*, No. e202303916. (g) Chen, J.; Zhang, R.; Ma, C.; Zhang, P.; Zhang, Y.; Wang, B.; Xue, F.; Jin, W.; Xia, Y.; Liu, C. Sustainable electrochemical dearomatization for the synthesis of diverse 2, 3-functionalized indolines. *Green Synth. Catal.* **2024**, *5*, 25–30. (h) Zhang, W.-Y.; Zhu, L.-H.; Cheng, Y.-Z.; You, S.-L. Construction of spirocyclic compounds via electrochemical intramolecular dearomatization of benzene derivatives. *Adv. Synth. Catal.* **2024**, *366*, 4205–4210. (i) Matsui, K.; Uyanik, M.; Ishihara, K. Electrochemical oxidative dearomatization of electron-deficient phenols using Br⁺/Br⁻ catalysis. *Chem. Commun.* **2025**, *61*, 2075–2078.
- (9) (a) Bertuzzi, G.; Ombrosi, G.; Bandini, M. Regio- and stereoselective electrochemical alkylation of Morita-Baylis-Hillman adducts. *Org. Lett.* **2022**, *24*, 4354–4359. (b) Rapisarda, L.; Fermi, A.; Ceroni, P.; Giovanelli, R.; Bertuzzi, G.; Bandini, M. Electroreductive C(sp³)-H functionalization of ethers via hydrogen-atom transfer. *Chem. Commun.* **2023**, *59*, 2664–2667. (c) Brunetti, A.; Bertuzzi, G.; Bandini, M. Catalyst and additive-free electrochemical CO₂ fixation into Morita-Baylis-Hillman acetates. *Synthesis* **2023**, *55*, 3047–3055. (d) Garbini, M.; Brunetti, A.; Pedrazzani, R.; Monari, M.; Marccaccio, M.; Bertuzzi, G.; Bandini, M. Electrochemical deeply reductive cyclodimerization of chalcones: exploring the “Self-adaptability” of galvanostatic eChem. *Chem. Commun.* **2024**, *60*, 404–407. (e) Brunetti, A.; Garbini, M.; Autuori, G.; Zanardi, C.; Bertuzzi, G.; Bandini, M. Electrochemical synthesis of itaconic acid derivatives via CO₂ fixation into allenenes. Expanding horizons in electrosynthesis through chemical divergency. *Chem. - Eur. J.* **2024**, *30*, No. e202401754.
- (10) (a) Pradhan, P.; Das, I.; Debnath, S.; Parveen, S.; Das, T. Synthesis of substituted tropones and advancement for the construction of structurally significant skeletons. *ChemistrySelect* **2022**, *7*, No. e202200440. (b) Brunetti, A.; Garbini, M.; Kub, N. G.; Monari, M.; Pedrazzani, R.; Zanardi, C.; Bertuzzi, G.; Bandini, M. Electrochemical site-selective alkylation of tropones via Formal C(sp³)-C(sp²) Coupling Reaction. *Adv. Synth. Catal.* **2024**, *366*, 1965–1971. (c) Brunetti, A.; Kiriakidi, S.; Garbini, M.; Monda, G.; Zanardi, C.; López, C. S.; Bertuzzi, G.; Bandini, M. Electrochemical nickel catalyzed C(sp²)-H functionalization of tropones with aldehydes. *ACS Catal.* **2025**, *15*, 3184–3190. (d) Garbini, M.; Moncullo, S.; Kiriakidi, S.; Melucci, M.; Bellini, S.; Zanardi, C.; Silva López, C.; Bertuzzi, G.; Bandini, M. Electrochemical chemo- and regioselective hetero-functionalization of tropones via C(sp²)-H derivatization. *Adv. Synth. Catal.* **2025**, *367*, No. e9592.
- (11) Zhuo, C.-X.; Zheng, C.; You, S.-L. Transition-metal-catalyzed asymmetric allylic dearomatization reactions. *Acc. Chem. Res.* **2014**, *47*, 2558–2573.
- (12) (a) Meier, T.; Braun, M. Tsuji–Trost allylic alkylation with ketone enolates. *Angew. Chem., Int. Ed.* **2006**, *45*, 6952–6955. (b) Meier, T.; Laicher, F.; Meletis, P.; Fidan, M.; Braun, M. Palladium-catalyzed diastereoselective and enantioselective allylic alkylations of ketone enolates. *Adv. Synth. Catal.* **2008**, *350*, 303–314. (c) Gräning, T.; Hartwig, J. F. Iridium-catalyzed regio- and enantioselective allylation of ketone enolates. *J. Am. Chem. Soc.* **2005**, *127*, 17192–17193. (d) Bélanger, É.; Cantin, K.; Messé, O.; Tremblay, M.; Paquin, J. F. Enantioselective Pd-catalyzed allylation reaction of fluorinated silyl enol ethers. *J. Am. Chem. Soc.* **2007**, *129*, 1034–1035. (e) Chen, M.; Hartwig, J. F. Iridium-catalyzed enantioselective allylic substitution of enol silanes from vinylogous esters and amides. *J. Am. Chem. Soc.* **2015**, *137*, 13972–13982.
- (13) (a) Nahra, F.; Macè, Y.; Lambin, D.; Riant, O. Copper/Palladium-Catalyzed 1,4 reduction and asymmetric allylic alkylation of α,β -unsaturated ketones: enantioselective dual catalysis. *Angew. Chem., Int. Ed.* **2013**, *52*, 3208–3212. (b) Nahra, F.; Macè, Y.; Boreux, A.; Billard, F.; Riant, O. Versatile Cu^I/Pd⁰ dual catalysis for the synthesis of quaternary α -allylated carbonyl compounds: development, mechanistic investigations and scope. *Chem. - Eur. J.* **2014**, *20*, 10970–10981.
- (14) (a) Trost, B. M.; Van Vranken, D. L. Asymmetric transition metal-catalyzed allylic alkylations. *Chem. Rev.* **1996**, *96*, 395–422. (b) Trost, B. M.; Crawley, M. L. Asymmetric transition-metal-catalyzed allylic alkylations: applications in total synthesis. *Chem. Rev.* **2003**, *103*, 2921–2944. (c) Lu, Z.; Ma, S. Metal-catalyzed enantioselective allylation in asymmetric synthesis. *Angew. Chem., Int. Ed. Engl.* **2008**, *47*, 258–297. (d) Trost, B. M.; Schultz, J. E. Palladium-catalyzed asymmetric allylic alkylation strategies for the synthesis of acyclic tetrasubstituted stereocenters. *Synthesis* **2019**, *51*, 1–30. (e) Pàmies, O.; Margalef, J.; Cañellas, S.; James, J.; Judge, E.; Guiry, P. J.; Moberg, C.; Bäckvall, J.-E.; Pfaltz, A.; Pericàs, M. P.; Diéguez, M. Recent advances in enantioselective Pd-catalyzed allylic substitution: from design to applications. *Chem. Rev.* **2021**, *121*, 4373–4505.
- (15) (a) Hong, A. Y.; Stoltz, B. M. The construction of all-carbon quaternary stereocenters by use of Pd-catalyzed asymmetric allylic alkylation reactions in total synthesis. *Eur. J. Org. Chem.* **2013**, *2013*, 2745–2759. (b) Yu, X.; Zhang, T.; Liu, J.; Li, X. Recent advances in the construction of quaternary stereocenters via palladium-catalyzed

decarboxylative asymmetric allylic alkylation. *Synthesis* **2021**, *53*, 4341–4352. (c) Süsse, L.; Stoltz, B. M. Enantioselective formation of quaternary centers by allylic alkylation with first-row transition-metal catalysts. *Chem. Rev.* **2021**, *121*, 4084–4099.

(16) (a) Trost, B. M.; Xu, J.; Schmidt, T. Palladium-catalyzed decarboxylative asymmetric allylic alkylation of enol carbonates. *J. Am. Chem. Soc.* **2009**, *131*, 18343–18357. (b) Pupo, G.; Properzi, R.; List, B. Asymmetric Catalysis with CO₂: The Direct α -allylation of ketones. *Angew. Chem., Int. Ed.* **2016**, *55*, 6099–6102.

(17) The beneficial use of a protic source was reported in a seminal Pd-catalyzed electrochemical allylation protocol Ding, W.; Li, M.; Fan, J.; Cheng, X. Palladium-catalyzed asymmetric allylic 4-pyridinylation via electroreductive substitution reaction. *Nat. Commun.* **2022**, *13*, 5642.

(18) For an exhaustive screening of protic sources, leaving groups on the allylating agents, and electrochemical conditions, see the [Supporting Information](#).

(19) Decreasing the current value to 5 mA (and thus prolonging the reaction time to 3 h) was found to be beneficial to avoid the overpotential generated by the higher resistivity caused by the low temperature.

(20) Trost, B. M.; Dong, G.; Vance, J. A. A diosphenol-based strategy for the total synthesis of (–)-terpestacin. *J. Am. Chem. Soc.* **2007**, *129*, 4540–4541.

(21) The increased chemical yield observed with water can be tentatively reconducted also to the known stabilizing effects exerted by the hydrogen bond network on radical anions: Tang, B.; Zhao, J.; Xu, J.-F.; Zhang, X. Tuning the stability of organic radicals: from covalent approaches to non-covalent approaches. *Chem. Sci.* **2020**, *11*, 1192–1204.

(22) (a) Furness, J. W.; Kaplan, A. D.; Ning, J.; Perdew, J. P.; Sun, J. Accurate and numerically efficient r2SCAN meta-generalized gradient approximation. *J. Phys. Chem. Lett.* **2020**, *11*, 8208–8215.

(b) Weigend, F. Accurate coulomb-fitting basis sets for H to Rn. *Phys. Chem. Chem. Phys.* **2006**, *8*, 1057–1065. (c) Weigend, F.; Ahlrichs, R. Balanced basis sets of split valences, triple zeta valence and quadruple zeta valence quality for H to Rn: Design and assessment of accuracy. *Phys. Chem. Chem. Phys.* **2005**, *7*, 3297–3305.

(d) Barone, V.; Cossi, M. Quantum calculation of molecular energies and energy gradients in solution by a conductor solvent model. *J. Phys. Chem. A* **1998**, *102*, 1995–2001.

(23) Amatore, C.; Jutand, A.; Meyer, G.; Mottier, L. Evidence of the reversible formation of cationic π -allylpalladium(II) complexes in the oxidative addition of allylic acetates to palladium(0) complexes. *Chem. - Eur. J.* **1999**, *5*, 466–473.

(24) In the DFT calculations, simple allyl acetate **2n** was chosen for the sake of simplicity. This reacts with the same regioselectivity as cinnamyl acetate **2a**.